Published in final edited form as:

J Cell Physiol. 2022 February ; 237(2): 1561–1572. doi:10.1002/jcp.30630.

Casein Kinase II Activates Bik to Induce Death of Hyperplastic Mucous Cells in a Cell Cycle-dependent Manner

Yohannes A. Mebratu[1], **Jewel Imani**[1], **Jane T. Jones**[2], **Yohannes Tesfaigzi**[1]

[1]Pulmonary and Critical Care Medicine, Brigham and Women's Hospital, Harvard Medical School, Boston, MA, USA.

[2]Department of Microbiology & Immunology Geisel School of Medicine at Dartmouth, Hanover, NH, USA

Abstract

Extensive inflammation causes epithelial cell hyperplasia in airways and Bcl-2-interacting killer (BIK) reduces epithelial cell and mucous cell hyperplasia without affecting resting cells to restore homeostasis. These observations suggest that Bik induces apoptosis in a cell cycle-specific manner, but the mechanisms are not understood. Mice were exposed to allergen for 3, 14, or 30 days and Bik expression was induced in airway epithelia of transgenic mice. Bik reduced epithelial and mucous cell hyperplasia when mice were exposed to allergen for 3 or 12 days, but not when exposure lasted for 30 days, and Ki67-positivity was reduced. In culture, Bik expression killed proliferating cells but not quiescent cells. To capture the stage of the cell cycle when Bik induces cell death, airway cells that express fluorescent ubiquitin cell cycle indicators (FUCCI) were generated that fluoresce red or green during the G0/G1 and S/G2/M phases of the cells cycle, respectively. Regardless of the cell cycle stage, Bik expression eliminated green-fluorescent cells. Also, Bik, when tagged with a blue-fluorescent protein, was only detected in green cells. Bik phosphorylation mutants at threonine 33 or serine 35 demonstrated that phosphorylation activated Bik to induce death even in quiescent cells. Immunoprecipitation and proteomic approaches identified casein kinase IIα to be responsible for phosphorylating and activating Bik to kill cells in S/G2/M. Because casein kinase 2 alpha (CKIIα) is expressed only during G2/M phase, we conclude that Bik activation in airway epithelial cells selectively targets hyperplastic epithelial cells, while leaving resting airway cells unaffected.

Keywords

airway epithelial cells; hyperplastic mucous cells; house dust mite allergen; cell cycle; resolution; phosphorylation; apoptosis; kinase

Corresponding authors: Yohannes Tesfaigzi, Pulmonary and Critical Care Medicine, Brigham and Women's Hospital, Harvard Medical School, 75 Francis Boston, MA, USA., ytesfaigzi@bwh.harvard.edu.

Author contributions

YAM and YT conceived the study; JJ, YM, JI conducted the experiments, Y.A.M., JJ, JI, and YT analyzed the data and drafted the manuscript.

Conflict of Interest Statement

The authors have no conflict of interest with the content of this manuscript.

Introduction

Repair of epithelial injury involves initial cell hyperplasia followed by removal of hyperplastic cells to restore homeostasis (Harris et al., 2005; Stout et al., 2007; Tesfaigzi et al., 2002). The removal of hyperplastic cells is a coordinated process that induces death of only hyperplastic cells while leaving the quiescent cells unaffected and ensures the maintenance of the epithelial barrier integrity, while eliminating cells that are no longer needed. However, the mechanisms of how the induction of apoptosis in selected hyperplastic cells occurs are largely unknown.

Hyperplastic cells may be specifically targeted as they are in the cycling phase and, cumulative data indicate that mechanisms governing the cell cycle and apoptosis are closely linked in a complex and context-dependent manner (King & Cidlowski, 1995; Nahle et al., 2002; Zinkel, Gross, & Yang, 2006). For example, the apoptosis-inducing ability of a variety of agents is greatly potentiated in cells that are arrested in late G1 or early S phases of the cell cycle (Meikrantz, Gisselbrecht, Tam, & Schlegel, 1994). Further, in human endothelial cells, apoptosis induced by deprivation of growth factors is associated with an upregulation of cyclin A-associated cyclin-dependent kinase 2 (cdk2) activity (Levkau et al., 1998).

When cells proliferate, the mitotic cell cycle progression is controlled by the activation or inactivation of a conserved family of serine/threonine protein kinases known as the cyclin-dependent kinases (cdks) (Morgan, 1995; Weinberg, 1995). CKII is a ubiquitous cyclic nucleotide-independent serine/threonine protein kinase that targets many cellular proteins including several nuclear proteins involved in growth regulation (Meek & Street, 1992; Pinna, 1990). The role of CKII is highly conserved, as CKII is also involved in the transition from G1/S to G2/M In yeast cells (Glover, 1998; Hanna, Rethinaswamy, & Glover, 1995; Pepperkok, Lorenz, Ansorge, & Pyerin, 1994). CKII-related kinases have been shown to phosphorylate apoptosis modulators such as p53 and c-Myc (Bousset et al., 1994; Hall, Campbell, & Meek, 1996; Hupp, Meek, Midgley, & Lane, 1992; Schuster, Prowald, Schneider, Scheidtmann, & Montenarh, 1999). Also p53 phosphorylation at Ser-392 mediates DNA damage-induced apoptosis (Blaydes & Hupp, 1998), suggesting the role of CKII-mediated phosphorylation in apoptotic cell death.

Several mechanisms have been proposed that link the cell cycle with the cell death process. The B-cell lymphoma 2 (Bcl-2) family of proteins are known to regulate apoptosis. However, they also affect cell cycle arrest, and cell cycle entry (Janumyan et al., 2003). Proteins that regulate cell cycle progression can also induce apoptosis under conditions in which cell cycle progression is not properly orchestrated (Evan, Brown, Whyte, & Harrington, 1995; Harbour & Dean, 2000). However, whether CKII has a role in Bik-induced cell death of hyperplastic cells is not clear.

Our previous studies showed that exposure to an allergen induces epithelial and mucous cell hyperplasia and the resolution of the hyperplastic cells during prolonged exposure to the allergen is mediated by IFN-γ activating signal transducer and activator of transcription 1 (STAT1) (Z. Q. Shi, M. J. Fischer, G. T. De Sanctis, M. Schuyler, & Y. Tesfaigzi, 2002). Bik, a Bcl-2 family member that has only the BH3 domain in common with the other Bcl-2

family members, mediates the IFN-γ-induced resolution of hyperplastic cells (Mebratu, Dickey, Evans, & Tesfaigzi, 2008). However, expression of Bik using adenoviral vectors (Mebratu, Schwalm, Smith, Schuyler, & Tesfaigzi, 2011) or using Bik-derived peptides (Mebratu et al., 2017) targets only hyperplastic mucous cells, while leaving the integrity of the epithelium intact. Therefore, the present study was focused on investigating whether Bik affects only proliferating cells. We examined the stage of the cell cycle that is most susceptible to Bik-induced cell death using fluorescent, ubiquitination-based cell cycle indicator (FUCCI) that is tagged with red- and green-fluorescent proteins to mark cells in the G0/G1 and S/G2/M phases, respectively. After verifying that Bik expression selectively kills cells in the S/G2/M phase, we found that in proliferating cells, Bik phosphorylation is required for its pro-apoptotic activation. Finally, we screened for kinases and found that CKII-α, expressed during the S/G2/M cell cycle stage, interacts and phosphorylates Bik at Thr33/Ser35 residues to promote epithelial cell death.

Materials and methods

Mice:

Pathogen-free male wild-type C57BL/6 were purchased from The Jackson Laboratory (Bar Harbor, ME). After a 14-day quarantine period, mice were entered into the experimental protocol at 8–10 weeks of age. The $bik^{-/-}$ mice, on C57BL/6 background, were provided by Andreas Strasser (Walter and Eliza Hall Institute, Melbourne, Australia). $Bik^{+/+}$ with $bik^{-/-}$ littermates were bred from the respective heterozygote mice at the Lovelace Respiratory Research Institute and genotyped (Coultas et al., 2004). Transgenic mice that conditionally express Bik in the respiratory epithelium were generated utilizing the reverse tetracycline-controlled transactivator (rtTA) expressed under the control of Clara cell secretory protein (CCSP) promoter (Mebratu et al., 2017). All mice were housed in isolated cages under specific pathogen-free conditions. During exposure to house dust mite (HDM) mice were kept with doxycycline-containing diet. All experiments were approved by the Lovelace Institutional Animal Care and Use Committee and were conducted at Lovelace Respiratory Research Institute, a facility approved by the Association for the Assessment and Accreditation for Laboratory Animal Care International.

Exposure to House Dust Mite (HDM):

HDM, from Dermatophagoides Pteronyssinus (Greer Laboratories, Lenoir, NC, lot #248041), purchased as 21.5 mg protein per 103.3 mg dry weight, was resuspended in sterile phosphate-buffered saline (PBS) and stored at −20 °C as frozen aliquots at a concentration of 1 μg/μl. For all HDM exposures, mice were anesthetized with isoflurane and exposed to HDM by intranasal instillation, both for the initial sensitization on days 1 and 8 and for the challenges for 3, 14, or 5 days per week over 30 d as described (De Vooght et al., 2009).

Lung Histology:

Preparation of lung tissues for histopathological examination was performed as previously described (Z. O. Shi, M. J. Fischer, G. T. De Sanctis, M. R. Schuyler, & Y. Tesfaigzi, 2002). Briefly, the left lungs were inflated and fixed at 25 cm pressure with zinc formalin and tissue sections stained with hematoxylin and eosin (H&E) and Alcian blue (AB) and periodic acid

Schiff (PAS) (Z. O. Shi et al., 2002). For quantifying epithelial cell hyperplasia (ECH) and mucous cell hyperplasia (MCH), the number of AB-positive cells and total cell counts per millimeter of basal lamina (BL) were quantified using the VisioMorph system (Visiopham, Horsholm, Denmark).

Immunofluorescent staining and image analysis:

Lung sections were deparaffinized, hydrated in graded ethanol and deionized water, washed in 0.05% Brij-35 in Dulbecco's PBS (pH 7.4), and then processed for immunostaining. Briefly, after antigen retrieval, sections were incubated for 30 min in 0.2% Triton X-100 with 0.2% saponin for antigen retrieval and then blocked using 3% IgG-free bovine serum albumin (BSA), 1% gelatin, and 2% normal donkey serum. After overnight incubation in a 1:500 dilution of anti-Bik antibodies (Cell Signaling Technology. Inc.) at 4 °C, immunolabeled cells were detected using F(ab)2 fragments of secondary Abs conjugated to Dylight-549 (Jackson Immuno-Research Laboratories, West Grove, PA) at 1:1000 dilution. Slides were mounted with DAPI-containing Fluormount-G (SouthernBiotech, Birmingham, AL) for nuclear staining. Immunofluorescence was imaged using Axioplan 2 microscope (Carl Zeiss, Inc., Thornwood, NY) with a Plan-Neofluor 403/0.75 air objective and a charge-coupled device camera (Hamamatsu Photonics, Hamamatsu, Japan) and the Slidebook 6.0 acquisition software (Intelligent Imaging Innovation, Denver, CO).

Real-time PCR analysis:

Total RNA was isolated from the lungs using Trizol (Molecular Research Center Inc, Cincinnati, OH). Bik messenger RNA (mRNA) levels were quantified as described previously (Schwalm et al., 2008) using ABI HT 7900 Real-Time polymerase chain reaction (PCR) system using TaqMan One-step RT-PCR Gene Expression kit (Life Technologies, Waltham, MA).

Cell culture and viruses.

HEK293T cells are a simian vacuolating virus 40 (SV40) large T antigen-expressing and highly transfectable derivative of HEK293 cells, which are derived from human embryonic kidney cells transformed with human adenovirus type 5 (ATCC, Gaithersburg, MD, USA). HEK293T cells were grown at 37°C, 5% CO_2 and air, in Dulbecco's modified Eagle medium containing 10% Hyclone bovine growth serum, 50 U/mL penicillin and 50 μg/mL streptomycin. AALEB cells are SV40ER/hTERT immortalized human bronchial epithelial cells and were provided by Dr. S. Randell (University of North Carolina, Chapel Hill, NC). AALEB cells were cultured in bronchial epithelial cell growth medium (Cambrex Bio Science) at 37°C, 5% CO_2, and air. Ad-BIK_{WT} and Ad-BIK_{L61G} have been previously described (Mebratu et al., 2008).

Plasmids.

The following plasmids were obtained from AddGene: Nuclear localized blue fluorescent protein (pEBFP2-Nuc), encoding the enhanced blue fluorescent protein with a nuclear localization signal; pMDG2, encoding VSV-G protein; pRev, encoding HIV-1 Rev protein and psPAX2 encoding HIV-1 GAG/POL. The plasmid mPlum was obtained from Clontech.

The mPlum coding sequence was amplified and cloned downstream of the first 20 amino acids (MVSKGEEVIKEFMRFKEHME) of human citrate synthase to localize it to the mitochondrial matrix, in the mammalian expression vector pcDßA, where its expression is driven by the CMV enhancer. The EBFP2 coding sequence was first amplified and cloned in the pcDßA Mem vector, downstream of the first 11 amino acids (MGCGCSSHPED) of human lymphocyte-specific protein tyrosine kinase (LCK) to localize it to the cell membrane; next, a 21 amino acid "2A" sequence (GSGEGRGSLLTCGDVEENPGP) from the Thosea asigna virus (TaV) was cloned downstream of Mem-EBFP2; finally, the complete sequence of human BIK was cloned after the terminal P of TaV 2A. The resulting construct, pcDßA MemEBFP2–2A-hBIK, expressed two cistrons in equimolar amounts, encoding MemEBFP2–2A and hBIK preceded by a single proline. Insert of both constructs were verified by sequencing. The G1-FUCCI (mKO2-$Cdt1_{30–120}$) and S/G2/M-FUCCI (mAG-$Geminin_{1–110}$) cassettes in the CSII-EF-MCS lentiviral vector were kindly provided by Dr. Miyawaki and colleagues. We received the BIK phospho-mutant expression plasmids (S33A and T35A) from Dr. G. Chinnadurai and the plasmid constructs expressing constitutively active phospho-mutants (S33D and T35D) were generated at Genscript (Genscript USA Inc.). Inserts of both constructs were verified by sequencing.

Transfection of HEK293T cells.

HEK293T cells, plated on 24-well rat-tail collagen-coated plates, were transfected by the calcium phosphate method with a total of 1 μg DNA consisting of pcDßA CitSyn-mPlum or empty vector, pcDßA, and effector plasmids (pcDßA Mem-EBFP2–2A, pcDßA Mem-EBFP2–2A-$hBIK_{WT}$ or pcDßA Mem-EBFP2–2A-$hBIK_{L61G}$) at equimolar concentrations in 400 μL of phenol red-free medium. After 24 h of transfection, cells were imaged for fluorescence using the mPlum (650 nm) and EBFP2 (448 nm) channels and at 20X for phase contrast.

Generation of FUCCI cell lines.

Ubiquitination-based cell cycle indicator (FUCCI) uses red- and green-emitting fluorescent proteins fused to E3 ligase substrates, Cdt1 and Geminin, to develop dual-color fluorescent probes that indicate whether individual cells are in the G_1 phase or the $S/G_2/M$ phases. Lentiviral expression vectors were generated by transfecting 5 million HEK293T cells in a 100 mm dish along with 5 μg of pMDG2, 5 μg of pRev and 5 μg of psPAX2 along with 10 μg of G_1-FUCCI and S/G_2/M-FUCCI lentiviral constructs. After 18 hours, cells were washed with PBS and incubated for another 24 hours in media before harvesting the supernatant containing FUCCI lentiviral particles. AALEB cells were plated and incubated for transduction with media containing the G1-FUCCI lentiviral particles in the presence of 1 μg/mL polybrene. After 16 hours, media was washed off and cells were allowed to propagate. The transduced cells were sorted for G1-FUCCI expression on a four-laser Beckman Coulter Legacy MoFlo (University of New Mexico Shared Resources Flow Cytometry Facility). The sorted G_1-FUCCI-AALEB cells were subsequently transduced with S/G_2/M-FUCCI lentiviral particles in the presence of 1 μg/mL polybrene, and similarly sorted for expression of S/G_2/M-FUCCI, resulting in FUCCI-AALEB cells (Supplement Fig. 1A). The same method was used to generate G_1-FUCCI-HEK293T cells and S/G_2/M-FUCCI-HEK293T cells (Supplement Fig. 1B).

Immunofluorescent staining and image analysis.

Lung sections were deparaffinized, hydrated in graded ethanol and deionized water, washed in 0.05% Brij-35 in Dulbecco's PBS (pH 7.4), and then processed for immunostaining. Briefly, after antigen retrieval, sections were incubated for 30 min in 0.2% Triton X-100 with 0.2% saponin for antigen retrieval and blocked using 3% IgG-free BSA, 1% gelatin, and 2% normal donkey serum. After overnight incubation in a 1:500 dilution of anti-Bik antibodies (Cell Signaling Technology. Inc.) at 4 °C, immunolabeled cells were detected using F(ab9)2 fragments of secondary Abs conjugated to Dylight-549 (Jackson Immuno-Research Laboratories, West Grove, PA) at 1:1000 dilution. Slides were mounted with DAPI-containing Fluormount-G (SouthernBiotech, Birmingham, AL) for nuclear staining. Immunofluorescence was imaged using Axioplan 2 microscope (Carl Zeiss, Inc., Thornwood, NY) with a Plan-Neofluor 403/0.75 air objective and a charge-coupled device camera (Hamamatsu Photonics, Hamamatsu, Japan) and the Slidebook 6.0 acquisition software (Intelligent Imaging Innovation, Denver, CO).

Real-time PCR analysis.

Total RNA was isolated from lungs using Trizol (Molecular Research Center Inc, Cincinnati, OH). Bik mRNA levels were quantified as described previously (Schwalm et al., 2008) using ABI HT 7900 Real Time-PCR system using TaqMan One-step RT-PCR Gene Expression kit (Life Technologies, Waltham, MA).

Live Cell Microscopy imaging.

Microscopy and time-lapse imaging of cell lines were performed on an Olympus IX81 with a Prior motorized stage and a custom-built incubation chamber (Applied Precision, Inc.). Chamber was kept between 35–36°C with 50% humidity using an attached Air-Therm ATX-H. Control and test cells were plated on a multi-well plate and imaged at the same time through 10X (UPLFLN 10XPH) or 20X (LUCPLFLN 20XPH) long-distance phase objectives using a C8484 Hamamatsu digital camera controlled by Metamorph v7.5 (Molecular Devices) acquisition software). FUCCI cells were transfected with EV, pcDßA MemEBFP2–2A-hBIK^{L61G}, or pcDßA MemEBFP2–2A-hBIK. Twenty-four h later cells were fixed and imaged by confocal microscopy (Olympus Fluoview, FV10i, Olympus Corporation). The proportion of cells in the G0/G1 or S/G2/M phase of the cell cycle that express MemEBFP2 were quantified and compared. Filter sets for fluorescence imaging were exciter 387/11, dichroic 409, emitter 447/60 for EBFP2; exciter 470/40, dichroic 495, emitter 520/35 for mAG; exciter 549/15, dichroic 565, emitter 585/29 for mKO2 and exciter 590/20, dichroic 605, emitter 647/57 for mPlum (values are in nm). Background correction for EBFP2 imaging used the background flattening function of Metamorph. Fiji open-source image processing software was used for post-processing and analysis of image data.

Statistical analysis.

Data were analyzed using statistical analysis software (Statistical Analysis Software Institute and GraphPad Prism). Data were expressed as mean with standard error from the mean (SEM), and differences between groups were assessed for significance by Student's t-test when the data were available in only two groups. When the data were available for more

than two groups, analysis of variance (ANOVA) was used to perform pair-wise comparison. When significant main effects were detected ($P < 0.05$), Fisher least significant difference test was used to determine the differences between groups. A P value of < 0.05 was considered to indicate statistical significance.

Results

Susceptibility of hyperplastic mucous cells to Bik-induced resolution after repeated challenges to allergen

The resolution of allergen-induced ECH and MCH during prolonged challenges to an allergen is abrogated in *bik*$^{-/-}$ mice (Mebratu et al., 2008). We investigated whether transgenic expression of Bik in airway epithelia reduces allergen-induced hyperplastic mucous cells after short or prolonged exposure to an allergen. When sensitized mice were challenged for 3 consecutive days, induction of Bik expression in airway epithelia of CCSP-rtTA/TetOBIK mice compared to CCSP-rtTA Bik-negative controls (Fig. 1A) reduced the number of hyperplastic airway epithelial cells (Fig. 1B) and hyperplastic mucous cells (Fig. 1C, D). Similar results were found when mice were challenged with HDM daily for 5 d/week over a period of two weeks (Supplementary Fig. S2A–F). However, when mice were challenged with HDM for 5 d/week over four weeks, although Bik was induced in the airways of the CCSP-rtTA/TetOBIK mice (Fig. 1E), neither the number of airway epithelial nor of mucous cells was reduced (Figs. 1F–H). Ki-67-positivity, a marker for the active phases of proliferation and not expressed in resting (quiescent) cells (Tompkins et al., 2011), in airway epithelia was 3-fold more in mice exposed for 2 compared with 4 weeks (Fig. 1I). This finding suggested that during prolonged exposure to allergen hyperplastic mucous cells become quiescent and resistant to Bik-induced death.

To better investigate the role of the cell cycle in Bik-induced cell death we followed confluent cultures of airway epithelial cells using time-lapse live-cell imaging and found that 10 hours after cells were infected with 100 multiplicity of infection (MOI) Ad-Bik death by extrusion of human airway epithelial cells occurred over a time course of 50 min (Fig. 2A). Further, the effect of 60% and 100% confluency on Bik-induced cell death was tested using AALEB cells, an immortalized but a non-transformed human airway epithelial cell line that stops replicating by contact inhibition (Supplement Fig. S3); thus, these cells are quiescent cells when they reach 100% confluency. At 50–60% confluency, these cells were treated with 50 ng/ml recombinant human FN-γ (rhIFN-γ) for 48 h. Viability was reduced only in proliferating (Fig. 2B) but not in confluent cultures (Fig. 2B). Increased IFN-γ concentrations did not affect cell viability at 100% confluency (Fig. 2C). Similarly, adenoviral expression of Bik (Ad-Bik) at 50–60% or 100% confluency showed that proliferating, but not confluent cultures were sensitive to Bik-induced cell death (Fig. 2D).

Preparation of HAECs that change fluorescence with cell cycle stage

FUCCI-AALEB cells that fluoresce red through G_0 and G_1 and green throughout the S, G_2, and M phases of the cell cycle (Supplement Fig. S1A, B) were enriched in S/G2/M by treating with 1 μM of aphidicolin over 0, 12, 24 and 48 h. At 24h, >80% of the cells

showed green fluorescence but the number of red-fluorescing cells started to increase at 48 h (Fig. 3A). The minimum aphidicolin dose with the highest percentage of cells arrested in $S/G_2/M$, and therefore, green fluorescence, and with minimal effect on cell viability over 24 h was determined to be the 1 μM aphidicolin concentration (Fig. 3B). Over a 24-h release from a cell cycle arrest with aphidicolin showed that green fluorescence ($S/G_2/M$) declined from 67% to 25% while red fluorescence (G_0/G_1) increased from 16% to 53% (Fig. 3C, panels b and c). Therefore, AALEB-FUCCI cells were synchronized for 24h with 1 μM aphidicolin treatment and subsequently infected with 100 MOI Ad-Bik at 0, 16, or 24 h. The percentages of cells that were fluorescing red and green and the fluorescence of cells undergoing nuclear condensation was monitored at the time of infection and at 16 and 24h. Regardless of when cells were infected following treatment with aphidicolin, more than 85% of the cells with green fluorescence but only 15% red-fluorescing cells showed condensed nuclei (Fig. 3D, E, F, and G). Time-lapse images of the cultures infected with Ad-Bik demonstrate that green cell undergo cell death and at the end predominantly red cells remain in culture (Supplemental Video). These findings demonstrate that cells die during the S/G2/M phase.

To firmly establish that Bik expression kills in G2/M, we generated expression constructs for wild-type and L61G-mutant Bik fused with the blue fluorescent protein EBFP2–2A targeted to the cell membrane (Mem-EBFP2). The 2A sequence derived from Thosea asigna virus (TaV) was inserted between the two open reading frames to facilitate the cleavage of the fused protein into two separated peptides, making Bik regain its function (Supplemental Fig. S4A). With increasing amount of Mem-EBFP2–2A-$hBIK_{L61G}$ expression, while keeping the mPlum transfection constant as control, the dose-dependent increase in the blue signal of Mem-EBFP2–2A along with the red signal for CitSyn-mPlum was visible (Supplemental Fig. S4B lower panels); however, the blue Mem-EBFP2 signal was weak or absent in cells expressing the Mem-EBFP2–2A-$hBIK_{WT}$ protein, and this was associated with progressively decreasing red signal of mPlum (Supplemental Fig. S4B upper panels). These results demonstrate that BIK_{WT} progressively killed cells when transfected as 100, 200, or 400 ng plasmid, limiting its expression (blue fluorescence) in the process. Transfection with the control plasmids expressing EBFP2–2A and mPlum verified that both fluorescent proteins are expressed and that EBFP2–2A is properly targeted to the cell membrane and mPlum to the mitochondria (Fig. 4A and Supplemental Fig. S4B). While co-transfection of Mem-EBFP2–2A-$hBIK_{L61G}$ and mPlum resulted in strong and properly targeted expression of EBFP2 and mPlum, expression of Mem-EBFP2–2A-$hBIK_{WT}$ resulted in the appearance of a very weak signal for EBFP2 and CitSyn-mPlum in rounded cells, consistent with apoptosis in cells expressing Mem-EBFP2–2A-$hBik_{WT}$ (Fig. 4A).

We used this tool to interrogate whether the blue signal of EBFP-2A-BIK was observed in FUCCI-AALEB cells during the green ($S/G_2/M$) or red (G_0/G_1) fluoresce stages of the cell cycle. Analysis of FUCCI-AALEB cells transfected with Mem-EBFP2–2A-$hBIK_{WT}$ showed that the percentage of cells with blue (BIK_{WT}-positive) and green fluorescence (in $S/G_2/M$) was reduced compared with blue ($hBIK_{WT}$-postiive) and red fluorescence (in G_0/G_1). However, in cells transfected with Mem-EBFP2–2A-$hBIK_{L61G}$ the numbers of blue- and red-fluorescing cells, representing cells in ($S/G_2/M$) and (G_0/G_1) phases, respectively, were similar (Fig. 4B). These findings were confirmed by fluorescence-activated cell

sorting (FACS) analyses of FUCCI-AALEB cells infected with HA-tagged Ad-BIK_{L61G} or Ad-BIK_{WT} expression constructs and analyzed at 16 and 24 h for percentages of cells fluorescing red (in G_0/G_1) and green (in $S/G_2/M$) (Fig. 4C). Within the cells infected with HA-AdBIK_{WT}, the percentage of cells in the $S/G_2/M$ compared with the G_0/G_1 phases of the cell cycle was reduced both at 16 and 24 h and cells transitioning to S were also reduced from 20 to 8 percent. However, this difference was not visible in the HA-AdBIK_{L61G} infected groups (Fig. 4C). Because Bik was equally expressed in red and green fluorescing cells, the loss of $S/G_2/M$ cells demonstrates that the blue-fluorescing Bik induced death during the S/G2/M phase of the cell cycle.

Bik requires phosphorylation by CKII for its apoptotic function

Cell cycle progression is controlled by phosphorylation of cyclin-dependent kinase (CDK) substrates (Fisher, Krasinska, Coudreuse, & Novak, 2012) and the apoptotic activity of Bik is dependent on the phosphorylation at Thr33 and Ser35 (Li et al., 2003; Verma, Zhao, & Chinnadurai, 2001). Because cyclin-dependent kinases could be important in activating Bik, we investigated whether Bik phosphorylation may trigger cell death of even quiescent, non-proliferating cells. Transfection of *BIK* knockout HEK293T cells at 60% confluency with empty vector or vectors expressing wild-type, T33A, or S35A phosphorylation-deficient Bik constructs showed that phospho-mutant Bik was deficient in causing cell death even in proliferating cells (Fig. 5A). In contrast, Bik T33D or S35D mutants that mimic constitutive phosphorylation reduced cell viability with the double mutant, T33D/S35D, being most effective (Fig. 5B). Further, both T33D and S35D mutants were effective in reducing cell viability even in confluent cultures, while the Bik_{WT} construct was ineffective (Fig. 5C). These findings indicated that Bik may be phosphorylated by a cell cycle-dependent kinase during the S/G2/M phase. To identify the kinase responsible for Bik phosphorylation, we first used a general proteomic approach by interrogating Bik/Bcl-2-interacting proteins. Therefore, protein extracts prepared from Bik-wild-type and -deficient HEK293 cells and $bik^{+/+}$ and $bik^{-/-}$ mouse airway epithelial cells were subjected to immunoprecipitation using Bcl-2 antibodies. Proteomic analyses of the immunoprecipitates from both human and mouse cells showed that casein kinase CKII was represented in Bik WT but not KO cells. Second, the primary amino acid sequence of Bik at the Thr33 and Ser35 are consensus CKII phosphorylation sites for BIK (Verma et al., 2001) (http://phospho.elm.eu.org). Therefore, we pre-treated HAECs with a CKII-specific inhibitor, TBB, and observed that Bik-induced cell death was blocked (Fig. 5D). Further, immunoprecipitation of HA-Bik followed by immunoblotting with anti-phospho-serine antibodies showed that the CKII inhibitors diminished Bik phosphorylation (Fig. 5E), further supporting the idea that CKII is responsible for activating Bik to induce cell death. TNF-α-induces CKII-dependent p65 phosphorylation at p65-Ser^{276} (Gang et al., 2015; Jacks & Koch, 2010). We found that TNF-α-induced p65 phosphorylation at S276 was inhibited when HAECs were treated with CKII-specific inhibitor, TBB (Fig. 5F), further supporting the observation that TBB inhibits the CKII-induced phosphorylation of Bik.

Discussion

The present study shows that Bik phosphorylation links the cell cycle to the apoptotic cell death machinery. The sensitivity of cells to Bik-induced cell death during S/G2/M rather than during the G0/G1 phase of the cell cycle was shown by various approaches: (1) Confluent cultures were resistant to death despite expressing high levels of Bik, (2) fluorescent labeling of cells as they progress through the cell cycle revealed that more than 80% of cells expressing Bik die during S/G2/M, and (3) expressed Bik, tagged by blue fluorescence or HA, is primarily detected in G0/G1 rather than in S/G2//M cells. Furthermore, casein kinase 2-α (CKII-α), a kinase that is expressed in G2/M, phosphorylated Bik to promote apoptotic activity.

When cells proliferate, the mitotic cell cycle progression is controlled by the activation or inactivation of a conserved family of serine/threonine protein kinases known as the cyclin-dependent kinases (cdks) (Morgan, 1997; Weinberg, 1995). CKII-α is localized in the cytoplasm during interphase but is distributed throughout the cell during mitosis as the alpha subunit is associated with spindle fibers during metaphase and anaphase. Therefore, the shuttling between the nucleus and the cytoplasm appears to play a significant role in its control of cell division (Yu, Spector, Bae, & Marshak, 1991).

The role of CKII is highly conserved, as CKII is also involved in the transition from G1/S to G2/M in yeast cells (Glover, 1998; Hanna et al., 1995; Pepperkok et al., 1994). CKII-induced phosphorylation at multiple p53 sites activates the sequence-specific DNA binding function of p53 (Hupp et al., 1992; Meek, Simon, Kikkawa, & Eckhart, 1990). Similarly, Cdc2 catalyzes the phosphorylation of the BH3-only protein BCL2 associated agonist of cell death (BAD) at Ser128 to activate BAD-mediated apoptosis and inhibiting the sequestration of growth factor-induced serine 136-phosphorylated BAD by members of the 14–3-3 family of proteins (Konishi, Lehtinen, Donovan, & Bonni, 2002). Further, overexpression of specific cdks or cyclin A in the presence of Bcl-2 increases the incidence of apoptosis (Meikrantz & Schlegel, 1996). CDK11^{p58} is also associated with apoptosis as a G2/M-specific protein kinase in breast cancer cells (Chi et al., 2014). CDK11^{p58} phosphorylates Bcl-2 at Ser70, Ser87 to enhance cyclohexamide-induced apoptosis in breast cancer cells (Yun et al., 2007). However, while Bik interacts with CKII-α, our immunoprecipitation analyses did not show evidence of Bik/CDK11^{p58} interaction, suggesting that different kinases may be important depending on the cell type.

Several approaches, including *in silico* analysis of the amino acid sequence representing consensus CKII phosphorylation sites, proteomic analyses of immunoprecipitates with anti-Bcl-2 antibodies of proteins from wild-type and Bik-deficient cells, and CKII inhibitor studies pointed to CKII-α phosphorylating Bik to cause death of HAECs. Previous studies have reported that T33 and/or S35 phosphorylation of Bik is crucial for its apoptotic activity in various human cancer cells (Li et al., 2003; Lin & Chen, 2017; Verma et al., 2001). Our data support those findings as mutation of these sites to alanine inhibited Bik from inducing cell death even in proliferating airway cells, while mutation to aspartate, to mimic constitutive phosphorylation, enabled Bik to cause cell death even in confluent cultures. These findings support the idea that resting cells of the airway epithelium are protected

and hyperplastic cells are targeted by Bik, likely because they express the CKII-α to activate Bik. Our findings in cultured cells suggest that kinase activity of CKII-α would be detected in hyperplastic cells in mouse airways, and these studies are under way to link this mechanism to the protection of resting cells in mouse airways from Bik-induced death.

When Bik expression is induced, it inactivates Bcl-2 from binding to Bcl-2-antagonist killer (Bak) and inositol triphosphate receptor (IP_3R) and thereby causes endoplasmic reticulum (ER) Ca^{2+} release and cell death (Mebratu et al., 2017). Therefore, cell cycle-dependent Thr33/Ser35 phosphorylation of Bik by CKII-α may modify the structure of Bik in a way that increases its affinity to Bcl-2 to a degree that Bik dissociates Bcl-2 from Bak and IP_3R and from other proteins to elicit cell death. More detailed structural analyses of Bik before and after Thr33/Ser35 phosphorylation are needed to fully elucidate how these modifications enhance Bik's affinity to Bcl-2.

Transgenic Bik expression in the airways was sufficient to reduce HDM-induced ECH and MCH when asthma was induced by challenging mice for 3-days or 2-weeks. However, increasing the HDM challenge period to four weeks rendered Bik ineffective in reducing both ECH and MCM, suggesting that when hyperplastic cells are present in airway epithelial over prolonged periods, they can become quiescent and form the regular long-lived cells that constitute the airway epithelium (Bruno & Darzynkiewicz, 1992). The mechanism of how the hyperplastic cells transition into a quiescent stage, as shown by the reduced detection of Ki-67-positive cells, is not clear. Bik expression in confluent cultures caused extrusion of apoptotic cells suggesting that there are some cells in S/G2/M phase of the cell cycle even in confluent cultures. When epithelial cells become too crowded several mechanisms can extrude out cells by inducing anoikis (Rosenblatt, Raff, & Cramer, 2001), and consistent with our observations, the extrusion process of epithelial cells requires cell cycle progression and occurs immediately after mitosis during the G2/M phase of the cell cycle (Anton, Kajita, Narumi, Fujita, & Tada, 2018).

In the current study, the dual-color fluorescent probes of FUCCI cells give us the opportunity to track whether cells are in G_1 phase or $S/G_2/M$ phases; however, this tool does not allow to specify whether the dying cells are specifically in S or G2/M phase. Future studies will design other markers that distinguish between the S and G2/M phases of the cell cycle. However, because casein kinase II is known to be specific for G2/M, we assume that cells are dying specifically during the G2/M phase of the cell cycle. Collectively, our findings suggest that Bik or Bik-derived peptides may be effective therapeutic tools to reduce hyperplastic mucous cells without destroying the integrity of the airway epithelium and its innate protective mechanism. Bik T33D/S35D as a therapeutic gene successfully treated pancreatic, lung and breast tumors in preclinical cancer models with virtually no toxicity (Lang et al., 2011; Sher et al., 2011; Xie et al., 2012; Xie et al., 2007). The fact that Bik targets specifically hyperplastic cells could be how Bik protects from cell transformation, but this feature may also minimize side-effects, supporting continued research in applying Bik and its derived peptides as a therapeutic approach in patients with asthmatic or chronic bronchitis.

Supplementary Material

Refer to Web version on PubMed Central for supplementary material.

Acknowledgment

We are grateful to Shayna Lucero at the University of New Mexico Shared Resources Flow Cytometry Facility for help in sorting cells and Susan Fort for genotyping of transgenic mice. These studies were supported by grants RO1HL068111 and R01HL140839 (to YT). Ms. Elise Bennett helped with the preparation of figures.

Data Availability Statement

The data that support the findings of this study are available from the corresponding author upon reasonable request.

References

Anton KA, Kajita M, Narumi R, Fujita Y, & Tada M (2018). Src-transformed cells hijack mitosis to extrude from the epithelium. Nat Commun, 9(1), 4695. doi:10.1038/s41467-018-07163-4 [PubMed: 30410020]

Blaydes JP, & Hupp TR (1998). DNA damage triggers DRB-resistant phosphorylation of human p53 at the CK2 site. Oncogene, 17(8), 1045–1052. doi:10.1038/sj.onc.1202014 [PubMed: 9747884]

Bousset K, Oelgeschlager MH, Henriksson M, Schreek S, Burkhardt H, Litchfield DW, … Luscher B (1994). Regulation of transcription factors c-Myc, Max, and c-Myb by casein kinase II. Cell Mol Biol Res, 40(5–6), 501–511. [PubMed: 7735324]

Bruno S, & Darzynkiewicz Z (1992). Cell cycle dependent expression and stability of the nuclear protein detected by Ki-67 antibody in HL-60 cells. Cell Prolif, 25(1), 31–40. doi:10.1111/j.1365-2184.1992.tb01435.x [PubMed: 1540682]

Chi Y, Wang L, Xiao X, Wei P, Wang Y, & Zhou X (2014). Abnormal expression of CDK11p58 in prostate cancer. Cancer Cell Int, 14(1), 2. doi:10.1186/1475-2867-14-2 [PubMed: 24397471]

Coultas L, Bouillet P, Stanley EG, Brodnicki TC, Adams JM, & Strasser A (2004). Proapoptotic BH3-only Bcl-2 family member Bik/Blk/Nbk is expressed in hemopoietic and endothelial cells but is redundant for their programmed death. Mol Cell Biol, 24(4), 1570–1581. [PubMed: 14749373]

De Vooght V, Vanoirbeek JA, Haenen S, Verbeken E, Nemery B, & Hoet PH (2009). Oropharyngeal aspiration: an alternative route for challenging in a mouse model of chemical-induced asthma. Toxicology, 259(1–2), 84–89. doi:10.1016/j.tox.2009.02.007 [PubMed: 19428947]

Evan GI, Brown L, Whyte M, & Harrington E (1995). Apoptosis and the cell cycle. Curr Opin Cell Biol, 7(6), 825–834. doi:10.1016/0955-0674(95)80066-2 [PubMed: 8608013]

Fisher D, Krasinska L, Coudreuse D, & Novak B (2012). Phosphorylation network dynamics in the control of cell cycle transitions. J Cell Sci, 125(Pt 20), 4703–4711. doi:10.1242/jcs.106351 [PubMed: 23223895]

Gang X, Wang Y, Wang Y, Zhao Y, Ding L, Zhao J, … Wang G (2015). Suppression of casein kinase 2 sensitizes tumor cells to antitumor TRAIL therapy by regulating the phosphorylation and localization of p65 in prostate cancer. Oncol Rep, 34(3), 1599–1604. doi:10.3892/or.2015.4123 [PubMed: 26165401]

Glover CV 3rd. (1998). On the physiological role of casein kinase II in Saccharomyces cerevisiae. Prog Nucleic Acid Res Mol Biol, 59, 95–133. doi:10.1016/s0079-6603(08)61030-2 [PubMed: 9427841]

Hall SR, Campbell LE, & Meek DW (1996). Phosphorylation of p53 at the casein kinase II site selectively regulates p53-dependent transcriptional repression but not transactivation. Nucleic Acids Res, 24(6), 1119–1126. doi:10.1093/nar/24.6.1119 [PubMed: 8604347]

Hanna DE, Rethinaswamy A, & Glover CV (1995). Casein kinase II is required for cell cycle progression during G1 and G2/M in Saccharomyces cerevisiae. J Biol Chem, 270(43), 25905–25914. doi:10.1074/jbc.270.43.25905 [PubMed: 7592778]

Harbour JW, & Dean DC (2000). Rb function in cell-cycle regulation and apoptosis. Nat Cell Biol, 2(4), E65–67. doi:10.1038/35008695 [PubMed: 10783254]

Harris JF, Fischer MJ, Hotchkiss JR, Monia BP, Randell SH, Harkema JR, & Tesfaigzi Y (2005). Bcl-2 sustains increased mucous and epithelial cell numbers in metaplastic airway epithelium. Am J Respir Crit Care Med, 171(7), 764–772. [PubMed: 15618464]

Hupp TR, Meek DW, Midgley CA, & Lane DP (1992). Regulation of the specific DNA binding function of p53. Cell, 71(5), 875–886. doi:10.1016/0092-8674(92)90562-q [PubMed: 1423635]

Jacks KA, & Koch CA (2010). Differential regulation of mitogen- and stress-activated protein kinase-1 and −2 (MSK1 and MSK2) by CK2 following UV radiation. J Biol Chem, 285(3), 1661–1670. doi:10.1074/jbc.M109.083808 [PubMed: 19933278]

Janumyan YM, Sansam CG, Chattopadhyay A, Cheng N, Soucie EL, Penn LZ, … Yang E (2003). Bcl-xL/Bcl-2 coordinately regulates apoptosis, cell cycle arrest and cell cycle entry. Embo J, 22(20), 5459–5470. doi:10.1093/emboj/cdg533 [PubMed: 14532118]

King KL, & Cidlowski JA (1995). Cell cycle and apoptosis: common pathways to life and death. J Cell Biochem, 58(2), 175–180. doi:10.1002/jcb.240580206 [PubMed: 7673325]

Konishi Y, Lehtinen M, Donovan N, & Bonni A (2002). Cdc2 phosphorylation of BAD links the cell cycle to the cell death machinery. Mol Cell, 9(5), 1005–1016. doi:10.1016/s1097-2765(02)00524-5 [PubMed: 12049737]

Lang JY, Hsu JL, Meric-Bernstam F, Chang CJ, Wang Q, Bao Y, … Hung MC (2011). BikDD eliminates breast cancer initiating cells and synergizes with lapatinib for breast cancer treatment. Cancer Cell, 20(3), 341–356. doi:10.1016/j.ccr.2011.07.017 [PubMed: 21907925]

Levkau B, Koyama H, Raines EW, Clurman BE, Herren B, Orth K, … Ross R (1998). Cleavage of p21Cip1/Waf1 and p27Kip1 mediates apoptosis in endothelial cells through activation of Cdk2: role of a caspase cascade. Mol Cell, 1(4), 553–563. [PubMed: 9660939]

Li YM, Wen Y, Zhou BP, Kuo HP, Ding Q, & Hung MC (2003). Enhancement of Bik antitumor effect by Bik mutants. Cancer Res, 63(22), 7630–7633. [PubMed: 14633680]

Lin ML, & Chen SS (2017). Activation of Casein Kinase II by Gallic Acid Induces BIK-BAX/BAK-Mediated ER Ca(++)-ROS-Dependent Apoptosis of Human Oral Cancer Cells. Front Physiol, 8, 761. doi:10.3389/fphys.2017.00761 [PubMed: 29033852]

Mebratu YA, Dickey BF, Evans C, & Tesfaigzi Y (2008). The BH3-only protein Bik/Blk/Nbk inhibits nuclear translocation of activated ERK1/2 to mediate IFNgamma-induced cell death. J Cell Biol, 183(3), 429–439. [PubMed: 18981230]

Mebratu YA, Leyva-Baca I, Wathelet MG, Lacey N, Chand HS, Choi AMK, & Tesfaigzi Y (2017). Bik reduces hyperplastic cells by increasing Bak and activating DAPk1 to juxtapose ER and mitochondria. Nat Commun, 8(1), 803. doi:10.1038/s41467-017-00975-w [PubMed: 28986568]

Mebratu YA, Schwalm K, Smith KR, Schuyler M, & Tesfaigzi Y (2011). Cigarette smoke suppresses Bik to cause epithelial cell hyperplasia and mucous cell metaplasia. Am J Respir Crit Care Med, 183(11), 1531–1538. [PubMed: 21317312]

Meek DW, Simon S, Kikkawa U, & Eckhart W (1990). The p53 tumour suppressor protein is phosphorylated at serine 389 by casein kinase II. Embo J, 9(10), 3253–3260. [PubMed: 2145148]

Meek DW, & Street AJ (1992). Nuclear protein phosphorylation and growth control. Biochem J, 287 (Pt 1), 1–15. doi:10.1042/bj2870001 [PubMed: 1417761]

Meikrantz W, Gisselbrecht S, Tam SW, & Schlegel R (1994). Activation of cyclin A-dependent protein kinases during apoptosis. Proc Natl Acad Sci U S A, 91(9), 3754–3758. [PubMed: 8170983]

Meikrantz W, & Schlegel R (1996). Suppression of apoptosis by dominant negative mutants of cyclin-dependent protein kinases. J Biol Chem, 271(17), 10205–10209. [PubMed: 8626584]

Morgan DO (1995). Principles of CDK regulation. Nature, 374, 131–134. [PubMed: 7877684]

Morgan DO (1997). Cyclin-dependent kinases: engines, clocks, and microprocessors. Annu Rev Cell Dev Biol, 13, 261–291. doi:10.1146/annurev.cellbio.13.1.261 [PubMed: 9442875]

Nahle Z, Polakoff J, Davuluri RV, McCurrach ME, Jacobson MD, Narita M, … Lowe SW (2002). Direct coupling of the cell cycle and cell death machinery by E2F. Nat Cell Biol, 4(11), 859–864. doi:10.1038/ncb868 [PubMed: 12389032]

Pepperkok R, Lorenz P, Ansorge W, & Pyerin W (1994). Casein kinase II is required for transition of G0/G1, early G1, and G1/S phases of the cell cycle. J Biol Chem, 269(9), 6986–6991. [PubMed: 8120061]

Pinna LA (1990). Casein kinase 2: an 'eminence grise' in cellular regulation? Biochim Biophys Acta, 1054(3), 267–284. doi:10.1016/0167-4889(90)90098-x [PubMed: 2207178]

Rosenblatt J, Raff MC, & Cramer LP (2001). An epithelial cell destined for apoptosis signals its neighbors to extrude it by an actin- and myosin-dependent mechanism. Curr Biol, 11(23), 1847–1857. [PubMed: 11728307]

Schuster N, Prowald A, Schneider E, Scheidtmann KH, & Montenarh M (1999). Regulation of p53 mediated transactivation by the beta-subunit of protein kinase CK2. Febs Lett, 447(2–3), 160–166. doi:10.1016/s0014-5793(99)00273-2 [PubMed: 10214938]

Schwalm K, Stevens JF, Jiang Z, Schuyler MR, Schrader R, Randell SH, … Tesfaigzi Y (2008). Expression of the pro-apoptotic protein bax is reduced in bronchial mucous cells of asthmatics. Am J Physiol Lung Cell Mol Physiol, 294(6), L1102–1109. [PubMed: 18390829]

Sher YP, Liu SJ, Chang CM, Lien SP, Chen CH, Han Z, … Hung MC (2011). Cancer-targeted BikDD gene therapy elicits protective antitumor immunity against lung cancer. Mol Cancer Ther, 10(4), 637–647. doi:10.1158/1535-7163.MCT-10-0827 [PubMed: 21282355]

Shi ZO, Fischer MJ, De Sanctis GT, Schuyler MR, & Tesfaigzi Y (2002). IFN-gamma, but not Fas, mediates reduction of allergen-induced mucous cell metaplasia by inducing apoptosis. J Immunol, 168(9), 4764–4771. [PubMed: 11971027]

Shi ZQ, Fischer MJ, De Sanctis GT, Schuyler M, & Tesfaigzi Y (2002). IFNg but not Fas mediates reduction of allergen-induced mucous cell metaplasia by inducing apoptosis. J Immunol, 168, 4764–4771. [PubMed: 11971027]

Stout BA, Melendez K, Seagrave J, Holtzman MJ, Wilson B, Xiang J, & Tesfaigzi Y (2007). STAT1 activation causes translocation of Bax to the endoplasmic reticulum during the resolution of airway mucous cell hyperplasia by IFN-gamma. J Immunol, 178(12), 8107–8116. doi:178/12/8107 [pii] [PubMed: 17548649]

Tesfaigzi Y, Fischer MJ, Daheshia M, Green FH, De Sanctis GT, & Wilder JA (2002). Bax is crucial for IFN-gamma-induced resolution of allergen-induced mucus cell metaplasia. J Immunol, 169(10), 5919–5925. [PubMed: 12421976]

Tompkins DH, Besnard V, Lange AW, Keiser AR, Wert SE, Bruno MD, & Whitsett JA (2011). Sox2 activates cell proliferation and differentiation in the respiratory epithelium. Am J Respir Cell Mol Biol, 45(1), 101–110. doi:10.1165/rcmb.2010-0149OC [PubMed: 20855650]

Verma S, Zhao LJ, & Chinnadurai G (2001). Phosphorylation of the pro-apoptotic protein BIK: mapping of phosphorylation sites and effect on apoptosis. J Biol Chem, 276(7), 4671–4676. [PubMed: 11084041]

Weinberg RA (1995). The retinoblastoma protein and cell cycle control. Cell, 81(3), 323–330. [PubMed: 7736585]

Xie X, Li L, Xiao X, Guo J, Kong Y, Wu M, … Xie X (2012). Targeted expression of BikDD eliminates breast cancer with virtually no toxicity in noninvasive imaging models. Mol Cancer Ther, 11(9), 1915–1924. doi:10.1158/1535-7163.MCT-12-0191 [PubMed: 22752427]

Xie X, Xia W, Li Z, Kuo HP, Liu Y, Li Z, … Hung MC (2007). Targeted expression of BikDD eradicates pancreatic tumors in noninvasive imaging models. Cancer Cell, 12(1), 52–65. doi:10.1016/j.ccr.2007.05.009 [PubMed: 17613436]

Yu IJ, Spector DL, Bae YS, & Marshak DR (1991). Immunocytochemical localization of casein kinase II during interphase and mitosis. J Cell Biol, 114(6), 1217–1232. doi:10.1083/jcb.114.6.1217 [PubMed: 1894695]

Yun X, Wu Y, Yao L, Zong H, Hong Y, Jiang J, … Gu J (2007). CDK11(p58) protein kinase activity is associated with Bcl-2 down-regulation in pro-apoptosis pathway. Mol Cell Biochem, 304(1–2), 213–218. doi:10.1007/s11010-007-9502-x [PubMed: 17516030]

Zinkel S, Gross A, & Yang E (2006). BCL2 family in DNA damage and cell cycle control. Cell Death Differ, 13(8), 1351–1359. doi:10.1038/sj.cdd.4401987 [PubMed: 16763616]

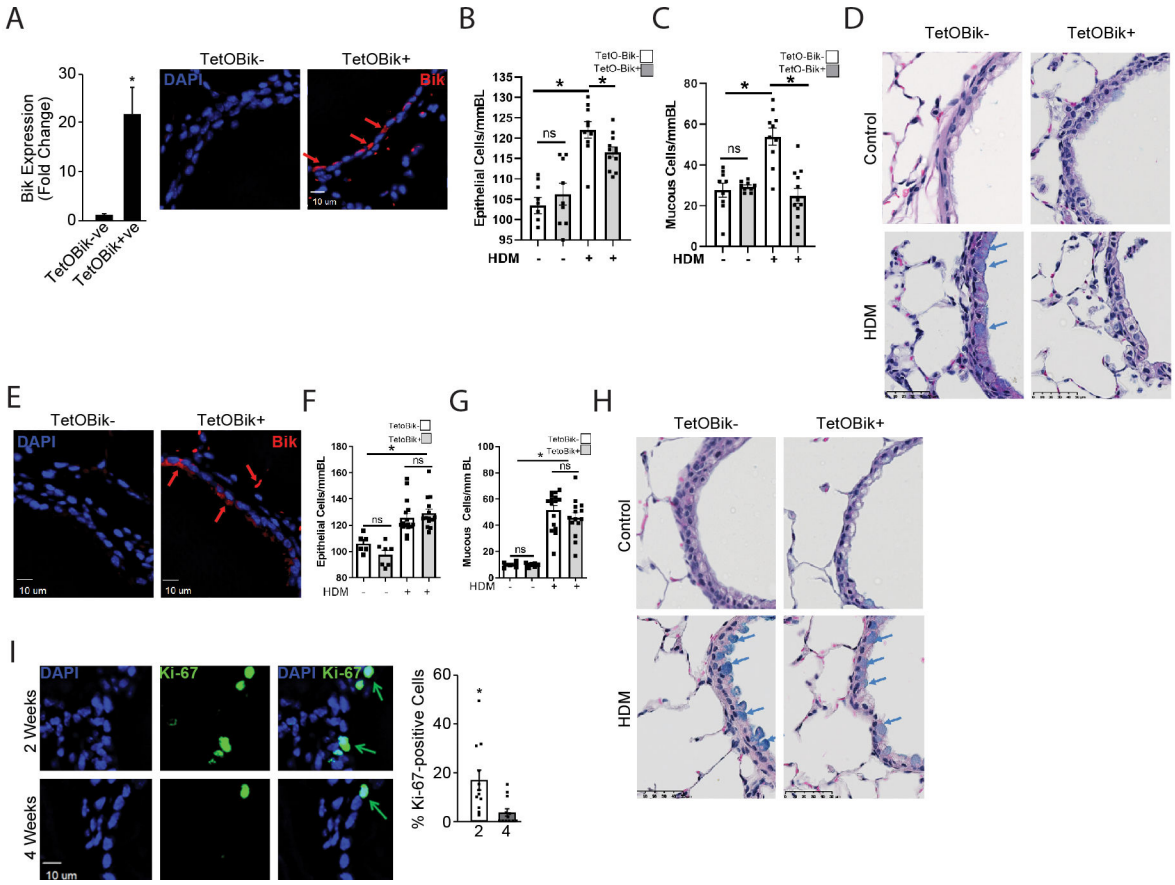

Figure 1. Transgenic expression of Bik reduces epithelial and mucous cell numbers following HDM challenge for three days.

(A, B, C, D) CCSP-rtTA and CCSP-rtTA, tetO-BIK mice were exposed via intranasal instillation to 50 μg HDM on days 1 and 8 and subsequently exposed via intranasal instillation with 50 μg HDM once a day on days 15–17. Mice were placed on Dox diet during days 15–17 and euthanized on day 20. Control groups were given vehicle only during the study period. **(A)** Expression of Bik analyzed by qPCR and immunostaining. AB/H&E-stained tissue sections from the left lung quantified for **(B)** total epithelial cells/mm BL and **(C)** total mucous cells/mm BL. **(D)** Representative images of AB H&E stained lung tissues. **(E, F, G, H)** CCSP-rtTA and CCSP-rtTA, tetO-BIK mice exposed via intranasal instillation to 50 μg HDM on days 1 and 8 and subsequently exposed via intranasal instillation to 50 μg HDM on days 15–19, 22–26, 29–33, and 36–40. Mice were placed on Dox diet during the entire 4 wks of challenge and euthanized on day 43. Control groups were given vehicle only during the study period. **(E)** Expression of BIK in the airways was analyzed by immunostaining. AB/H&E-stained tissue sections from the left lung were quantified for **(F)** total epithelial cells/mm BL and **(G)** total mucous cells/mm BL. **(H)** Representative images of AB H&E stained lung tissues. **(I)** Lung tissues of WT mice exposed to HDM for 2 or 4 weeks were immunostained using anti-Ki-67 antibody and percent Ki-67 positive cells in the airways quantified. Error bars indicate ± SEM, (n = 6 mice/group from N=2 experimental repeats); *indicates significant differences compared to the CCSP-rtTA control group. $P < 0.05$.

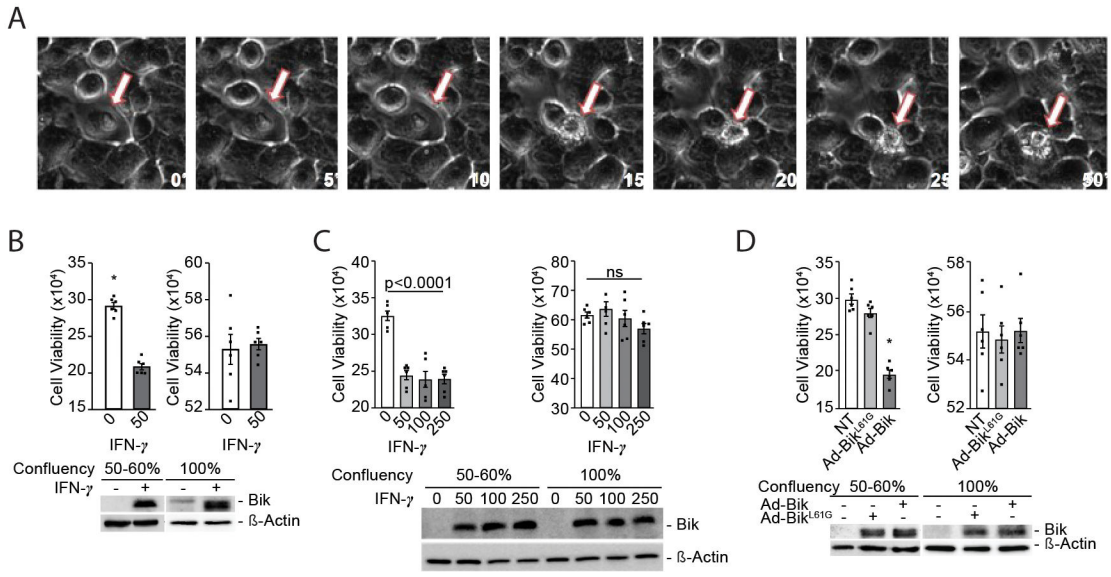

Figure 2. Only proliferating airway epithelial cells are sensitive to IFNγ- or Ad-Bik-induced cell death.

(A) Primary human AECs (HAECs) undergoing cell death were observed by live-cell imaging following infection with 100 MOI Ad-Bik. **(B)** HAECs were treated with 0 or 50 ng/ml rhIFN-γ at 50–60% or 100% confluency and harvested 48 h later and quantified for viability by trypan blue exclusion assay. Protein lysates were analyzed for Bik expression by Western blotting. **(C)** HAECs were treated with 0–250 ng/ml rhIFN-γ at 50–60% or 100% confluence and harvested 48 h later and quantified for viability by trypan blue exclusion assay. Protein lysates were analyzed for Bik expression by Western blotting. **(D)** HAECs were left untreated (NT) or were infected with 100 MOI Ad-Bik or Ad-Bik^{L61G} at 50–60% or 100% confluence. Cells were harvested 24 h later and quantified for viability by trypan blue exclusion assay. Protein lysates were analyzed for BIK expression by Western blotting. Data presented are means ± SEM for n=6 independent experiments per group and N=2 experimental repeats.

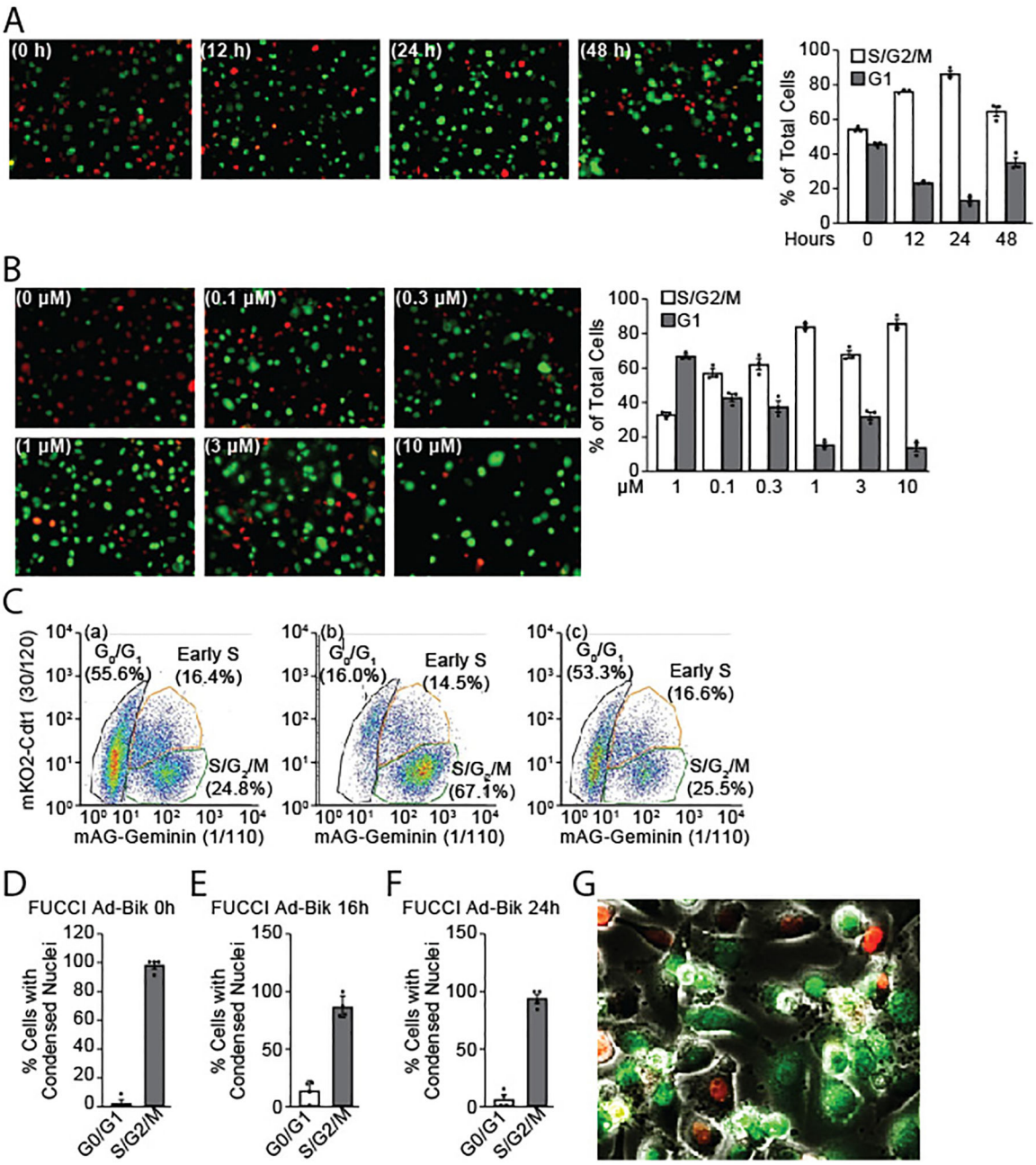

Figure 3. Bik induces cell death in AALEB cells during S/G2/M.

(A) Representative **f**luorescence images of FUCCI-AALEBs cells at various time-points post 1 μM of aphidicolin treatment for 0, 12, 24, and 48 h to arrest cells at G1/S. Red (G0/G1) and green (S/G2/M) cells at the time points post-treatment were quantified. **(B)** Representative fluorescent images of FUCCI-AALEBs cells 24 h post treatment with various doses of 0, 0.1, 0.3, 1, 3 and 10 μM aphidicolin. Quantification of red (G0/G1) and green (S/G2/M) cells at 24 h post-treatment. **(C)** Analysis of red and green fluorescence cells that were untreated (**panel a**), and after release from a 24-h long 1 μM of aphidicolin treatment at 0 h (**panel b**) and 24 h (**panel c**) by culturing them in media without aphidicolin. **(D)** AALEB-FUCCI were treated with 1 μM aphidicolin and infected with

100 MOI Ad-Bik at 0 **(D)**, 16 **(E)**, or 24 h **(F)** following aphidicolin treatment. Cells were washed and time-lapse images were recorded every 30 minutes for 24 h. Percent cells that were fluorescing green (S/G2/M) or red (G0/G1) of the total dead cells were quantified from the time lapse images. **(G)** A representative image of AALEB-FUCCI cells treated with aphidicolin and infected with Ad-Bik 24 h later. Data presented are means ± SEM for n=3 independent experiments per group and N=2 experimental repeats.

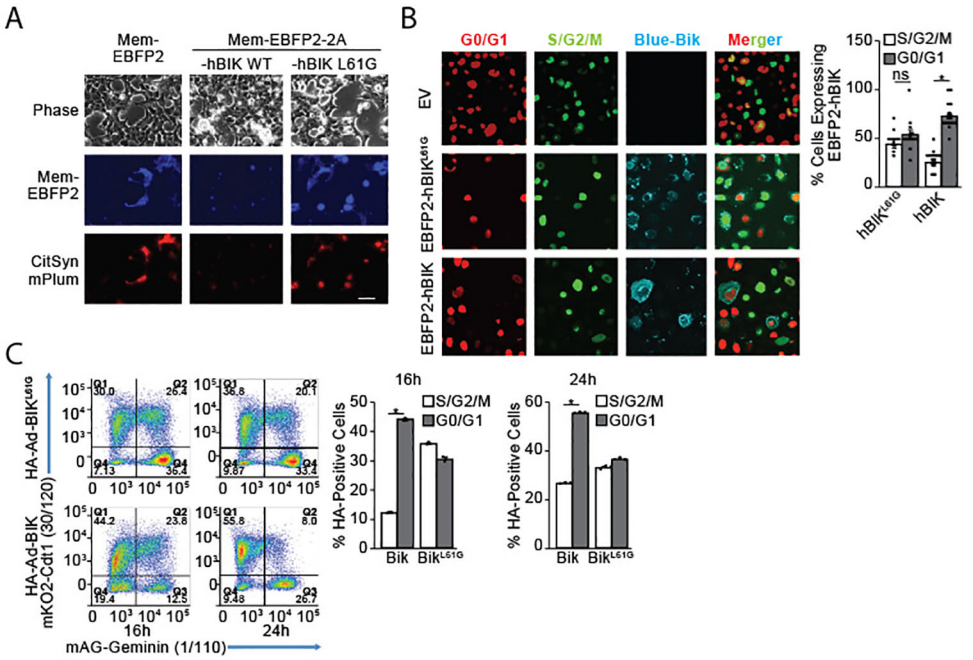

Figure 4. Bik expression and viability of cells during G0/G1 and S/G2/M.

(A) HEK293T cells in 24-well plates were transfected with pcDßA CitSyn-mPlum, and 400 ng pcDßA MemEBFP2–2A-hBIK or MemEBFP2–2A-hBIK^{L61G}. After 27 h, cells were imaged using phase contrast and in the mPlum (650 nm) and EBFP2 (448 nm) channels by confocal microscopy. **(B)** FUCCI-AALEB cells were transfected with Mem-EBFP2–2A-hBIK$_{WT}$ or Mem-EBFP2–2A-hBIK$_{L61G}$ and the percentage of cells expressing EBFP2-hBIk in green fluorescence (in S/G_2/M) or red fluorescence (in G_0/G_1) was analyzed by confocal microscopy. **(C)** After 16 and 24 h post Ad-HA-Bik$_{WT}$ or Ad-HA-Bik$_{L61G}$ infection, the percentage of FUCCI-AALEB cells expressing HA and fluoresce red (G0/G1) or green (S/G2/M) were quantified by FACS analysis. Data presented are means ± SEM; n = 6 independent experiments per group from N=2 experimental repeats.

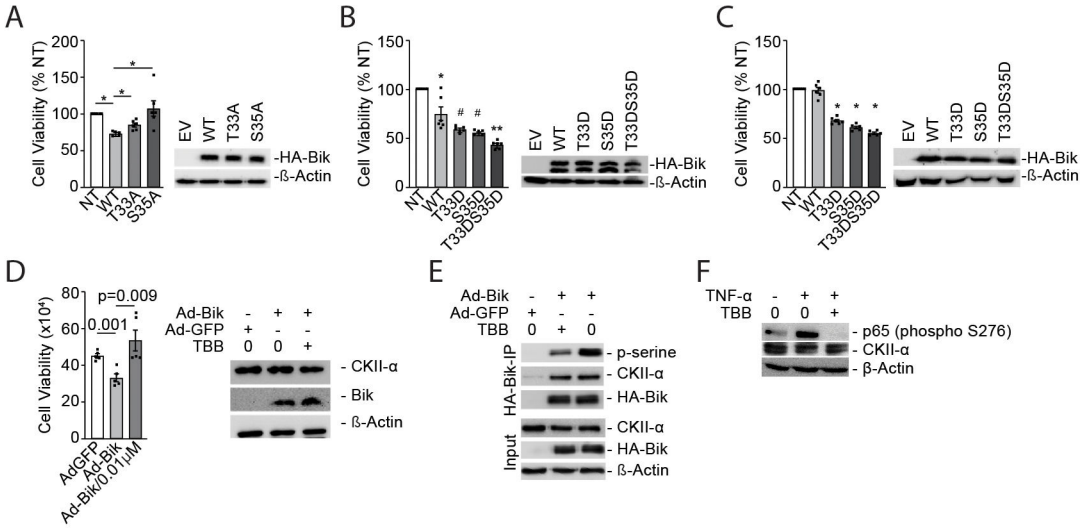

Figure 5. T33/S35 are phosphorylated by CK-IIα to activate Bik.

(A) Bik-deficient HEK293T cells were transfected with expression plasmids for wild-type, T33A, or S35A mutant Bik proteins at 60% confluence and cell viability quantified and Bik expression analyzed 27 h later by Western blotting. **(B)** Bik-deficient HEK293T cells were transfected with wild-type, T33D, S35D, or T33DS35D mutant expression plasmids at 60% confluency or **(C)** 100% confluency and cell viability quantified; Bik levels were quantified by Western blotting 27 h later. **(D)** HAECs were treated with mock or 10 nM casein kinase II inhibitor (TBB) and infected with 100 MOI Ad-GFP or Ad-Bik. Cells were quantified 24 h later and protein lysates were analyzed for the expression of Bik and casein kinase II alpha by Western blotting. **(E)** HAECs were treated with mock or 10 nM casein kinase II inhibitor (TBB) and infected with 100 MOI Ad-HA-Bik. Twenty-four hours later, protein lysates were immunoprecipitated with anti-HA antibody and probed for phospho-serine using anti-phospho-serine antibodies to determine Bik phosphorylation. **(F)** HAECs were treated with mock or 10 nM casein kinase II inhibitor (TBB) and treated with 20 ng/ml TNF-α for 30 minutes. Protein lysates were analyzed for p65 phosphorylation using anti-p65 phospho-serine 276 antibodies by Western blotting. Error bars indicate ± SEM; n = 6 independent experiments per group from N=2 experimental repeats; *indicates significant differences $P < 0.05$.